Hindawi
Mathematical Problems in Engineering
Volume 2020, Article ID 4247904, 9 pages
https://doi.org/10.1155/2020/4247904

*Research Article*

# Theoretical Model for Prediction of Turning Resistance of Tracked Vehicle on Soft Terrain

**Zhao Ding, Yaoming Li, and Zhong Tang**

*Key Laboratory of Modern Agricultural Equipment and Technology, Ministry of Education, Jiangsu University, Zhenjiang, Jiangsu 212013, China*

Correspondence should be addressed to Zhao Ding; dingzhao0806@foxmail.com

Received 21 October 2019; Revised 16 January 2020; Accepted 15 February 2020; Published 20 March 2020

Academic Editor: Ramon Sancibrian



Skid-steered tracked vehicles are commonly used in soft agricultural terrain due to its low ground pressure between vehicle tracks and the ground. However, the sliding and sinkage of the track during a turning maneuver causes considerable turning resistance, which reduces the vehicle's turning ability. Therefore, we constructed a theoretical model that predicts the turning resistance of tracked vehicles—under steady-state conditions on soft terrain—accounting for track sinkage effects and track slip and skid. The results demonstrate that the moment of turning resistance decreases with increased track slip and skid ratio but increases with track sinkage depth. The model-predicted moments of turning resistance for the outer and inner tracks—at a given track sinkage depth and track slip and skid ratio—are in reasonably close agreement with available experimental data. This theoretical model can be employed as a predictor for testing the turning resistance of tracked vehicles operating on a wide range of soils.

## 1. Introduction

Because they are capable of traversing a wide variety of soft terrain due to the low contact pressure between their track and ground, skid-steered tracked vehicles are widely used in agriculture [1–4]. However, in weak agricultural terrain, such as a paddy field, the soil is too soft because of the inordinately high water content. Because of such soft soil, the tracks sink deeply into the ground, causing the tracks to shear and bulldoze the terrain beneath them, which in turn causes track sinkage and a subsequent large turning resistance [5–9]. Furthermore, vehicles turning on soft terrain usually have a reduced tuning ability from the large degree of track sliding, which is evident in the slip and skid of the outer and inner tracks, respectively [10, 11]. These factors in combination often cause tracked vehicles to be immobilized when turning on soft terrain. If designers consider track sinkage effects and track slip and skid, those designers can predict the turning resistance of tracked vehicles under soft terrain conditions, and they can optimize their selection of design parameters and vehicle turning modes.

## 2. Background Theory

*2.1. Estimation of Turning Resistance of Tracked Vehicle from Coulomb's Law of Friction.* The track-ground interaction is important for predicting the turning resistance of tracked vehicles. In most previous studies, the shear force on the track-ground interface has been assumed to obey Coulomb's law of friction, where the coefficient of friction has been either isotropic or anisotropic. Steeds [12] conducted a systematic study of the steering behavior of tracked vehicles on firm ground. In his pioneering analysis, the coefficient of friction was isotropic, and the frictional force was acting opposite to the relative motion of the track with respect to the ground. In Steeds' study, the turning resistance could be predicted by calculating the equilibrium equations that were established under the assumption of steady-state turning. Subsequently, based on Steeds' study, Kitano and Jyozaki [13] constructed a prediction model that considered the friction to be anisotropic, and the friction coefficients along the longitudinal and lateral directions, $\mu_y$ and $\mu_x$, respectively, were derived from the pull-slip relation for a track in contact with the ground:

$$\mu_y = E_1\left(1 - e^{-E_2 i_y}\right),$$
$$\mu_x = E_1\left(1 - e^{-E_2}\right), \tag{1}$$

where $E_1 = 0.44$ and $E_2 = 20.0$ for a representative hard ground, and $i_y$ is track slip ratio along the longitudinal direction. Their estimation results were later substantiated from field measurements by Ehlert et al. [14]. Similar to Kitano and Jyozaki's model, Crosheck [15] provided a steady-state turning model for tracked vehicles on soft ground. In Crosheck's model, the friction between the track and ground was assumed to be anisotropic. The friction coefficient $\mu_y$ along the longitudinal direction was estimated using the "pull-slip" equation as follows:

$$\mu_y = E_1\left(1 - e^{E_2 C_{nj}}\right)\left(1 - e^{E_3 C_{nj} i_y}\right), \tag{2}$$

where $E_1$, $E_2$, and $E_3$ are derived from the pull-slip test of the track on the soft ground and are 0.95, −0.1, and −1.0 for the particular track on the specific ground, respectively [15], and $i_y$ is track slip ratio along the longitudinal direction. Whereas in the lateral direction, due to the full skid being assumed, the lateral coefficient of friction $\mu_x$ is equal to the value of $\mu_y$ at $i_y = 1$, and the $C_{nj}$ can be expressed as follows:

$$C_{nj} = \frac{CbL}{W_j}, \tag{3}$$

where $C$ is the cone index of the soil, $b$ is the track width, $L$ is the track contact length, and $W_j$ is the normal load acting on the track.

In the above models, the track-ground interaction is viewed as a Coulomb friction force. The strength of this approach is its simplicity. However, it has been determined to deliver insufficiently accurate predictions for the turning resistance of the tracked vehicle on the soft ground [16, 17]. As discussed by Guo [6], several reasons may be responsible for this phenomenon. First, this approach assumes that all points on the track-ground interface experience plastic deformation; however, it is not true when the turning radius of the tracked vehicle is large. Second, this approach does not consider the aggregation of shear displacement at the contact surface and the corresponding shear stress, which may be an oversimplification in soft terrains. Hence, the large discrepancy from test results on soft terrains may happen. Third, in this approach, the resistance coefficients in the longitudinal and lateral directions are constants, causing conflicts with Wong's theory that these coefficients vary with both the vehicle's turning radius and traffic speed [17].

*2.2. Estimation of Turning Resistance of Tracked Vehicle from Wong's General Theory.* Wong [17] developed a general theory that expanded Steeds' pioneering work. This general theory was derived from a detailed analysis of the relationship between shear stress and shear displacement in the track-ground interaction.

In Wong's model, as evident in Figure 1, the shear forces $dF_{o,i}$ at any point on the track-soil interface was assumed to have a direction opposite to that of the sliding

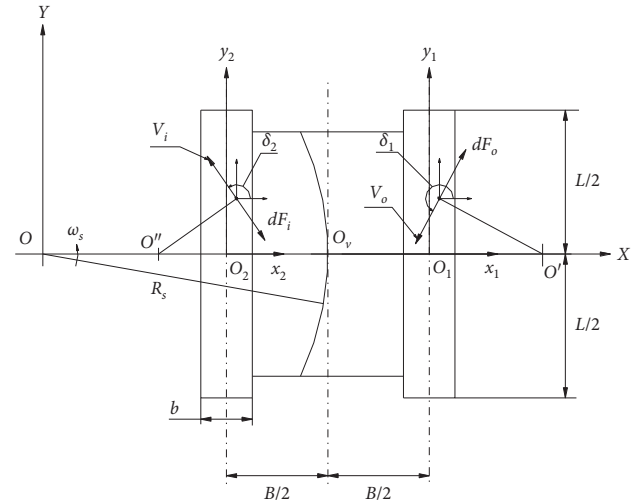


Figure 1: Kinematics of the tracked vehicle during a steady-state turn.

velocity of that point with respect to the ground. Then the shear stress $\tau$ at any point was described by the following exponential equation.

$$\tau = p\mu\left(1 - e^{-j/k}\right), \tag{4}$$

where $p$ is the normal pressure, $\mu$ is the coefficient of friction between the track and ground, and $k$ is the shear deformation parameter of the ground. The shear stress $\tau$, initially increases with increases in the shear displacement $j$ and subsequently approaches a constant value when the shear displacement reaches its maximum increase.

The shear displacement $j_{o,i}$ at a point on the outer and inner tracks that are in contact with the ground in the $X$ and $Y$ directions, with respect to a fixed frame of reference $XOY$, can be expressed as follows:

$$j_{X_{o,i}} = \left(R_s + \frac{B}{2} + x_{1,2}\right)\left\{\cos\left[\frac{\left(L/2 - y_{1,2}\right)\omega_s}{r\omega_{o,i}}\right] - 1\right\} - y_{1,2}\sin\left[\frac{(L/2 - y_1)\omega_s}{r\omega_{o,i}}\right], \tag{5}$$

$$j_{Y_{o,i}} = \left(R_s + \frac{B}{2} + x_{1,2}\right)\sin\left[\frac{\left(L/2 - y_{1,2}\right)\omega_s}{r\omega_{o,i}}\right] - \frac{L}{2} + y_{1,2}\cos\left[\frac{\left(L/2 - y_{1,2}\right)\omega_s}{r\omega_{o,i}}\right], \tag{6}$$

respectively, where $L$ is the track length, $B$ is the track tread, $\omega_s$ is the yaw velocity of the vehicle about the turning center $O$, $R_s$ is the turning radius of the vehicle about the center $O$, $r$ is the sprocket radius, and $\omega_o$ and $\omega_i$ are the sprocket angular velocities of the outer and inner tracks, respectively. Given the shear displacements in the $X$ and $Y$ directions, the resultant shear displacement $j_{o,i}$ can be expressed as follows:

$$j_{o,i} = \sqrt{j_{X_{o,i}}^2 + j_{Y_{o,i}}^2}. \tag{7}$$

Given the shear forces $dF_{o,i}$ on some element $dA$ of outer and inner tracks, the forces and moments acting on a tracked vehicle during a steady-state turn can then be calculated by an integral method. As evident in Figure 1, the component of the shear forces $dF_{o,i}$ along the longitudinal direction of the track constitutes the driving force or braking effort, while the shear forces $dF_{o,i}$ along the lateral component forms the lateral resistance. The resistance forces $F_{x(o,i)}$ acting on the lateral direction of the inner and outer tracks are as follows:

$$F_{X(o,i)} = -\int_{-L/2}^{L/2}\int_{-b/2}^{b/2} \tau_{o,i}\left(1 - e^{-j_{o,i}/K}\right) \times \cos\delta_{o,i}\,\mathrm{d}x\,\mathrm{d}y. \quad (8)$$

Given the resistance forces $F_{x(o,i)}$, as evident in Figure 2, the moments of turning resistance $M_{T(o,i)}$ from the lateral forces acting on the outer and inner tracks with respect to $O_1$ and $O_2$, respectively, can then be expressed as follows:

$$M_{T(o,i)} = -\int_{-L/2}^{L/2}\int_{-b/2}^{b/2} y\tau_{o,i}\left(1 - e^{-j_{o,i}/K}\right) \times \cos\delta_{o,i}\,\mathrm{d}x\,\mathrm{d}y. \quad (9)$$

where $\cos\delta_{o,i}$ is defined as follows:

$$\cos\delta_{o,i} = \frac{-y\omega_s}{\sqrt{\left[\left(R_s + B/2 + x\right)\omega_s - r\omega_{o,i}\right]^2 + \left(y\omega_s\right)^2}}. \quad (10)$$

Wong proposed a new method for the analysis of the turning behavior of tracked vehicles on firm ground. His method was based on the detailed analysis of the relationship between shear stress and shear displacement in the track-ground interaction and was demonstrated to be more accurate than previous models [17]. Wong's general theory was also demonstrated to be applicable to soft terrains [18, 19]. The formula proposed by Janosi and Hanamoto [20] can be expressed as follows:

$$\tau_{o,i} = (c + \sigma\tan\phi)\left(1 - e^{-j_{o,1}/k}\right), \quad (11)$$

where $c$ is the cohesion of soil, $\phi$ is the angle of soil internal shearing friction, and $\sigma$ is the normal stress exerted on the soil. By replacing equation (5) with equation (11), we can calculate the moments of turning resistance $M_{T(o,i)}$ without using any coefficient of resistance. However, the effect of vehicle track sinkage has yet to be considered.

Thus, this paper analyzes track sinkage effects and track slip and skid on the turning resistance of a tracked vehicle on soft terrain. Based on Wong's general theory, we established a theoretical model for the prediction of the moment of turning resistance of a tracked vehicle under different soil conditions, at given values of track sinkage depth, track slip ratio, and track skid ratio. Furthermore, to verify the validity of the prediction model, we conducted an experiment on the turning performance of a tracked harvester on paddy soil. To simplify the model, the following assumptions were made.

(1) The tracked vehicle is operating in a horizontal plane and has a steady-state turn.

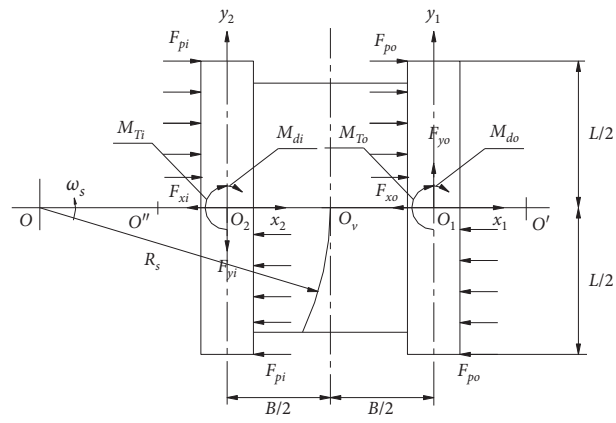


Figure 2: Forces and moments acting on a tracked vehicle during a steady-state turn.

(2) The longitudinal and lateral load transfers caused by the centrifugal force during the vehicle's turn are absent.

(3) The sliding-sinkage effect (i.e., an increase of track sinkage and motion resistance due to the track sliding) of the track and friction forces between the moving parts of the tracked undercarriage are absent.

## 3. Materials and Methods

### 3.1. Model Development

*3.1.1. Track Slip and Skid.* As illustrated in Figure 3, during the turn of a tracked vehicle, a braking force is exerted on the inner track, and a thrust force is exerted on the outer track. These two forces result in the slip of the outer track and skid of the inner track. For the outer track, this slip means that the theoretical velocity of the outer track *Uo* is greater than its actual velocity *Vo*. For the inner track, its skid means that the theoretical velocity of the inner track *Ui* is lower than its actual velocity *Vi*. To quantitatively describe track slip and skid, the slip ratio σo of the outer track and skid ratio σi of the inner track were defined according to equations (12) and (13), respectively.

$$\sigma_o = \frac{U_O - V_O}{U_O}, \quad (12)$$

$$\sigma_i = \frac{V_i - U_i}{V_i}. \quad (13)$$

The theoretical velocity of the outer track $U_o$, and the theoretical velocity of the inner track $U_i$ can be expressed by equations (14) and (15), respectively.

$$U_o = r\omega_o, \quad (14)$$

$$U_i = r\omega_i, \quad (15)$$

where $r$ *is* sprocket radius, $\omega_o$ is the sprocket angular velocity of the outer track, and $\omega_i$ is the sprocket angular velocity of the inner track.

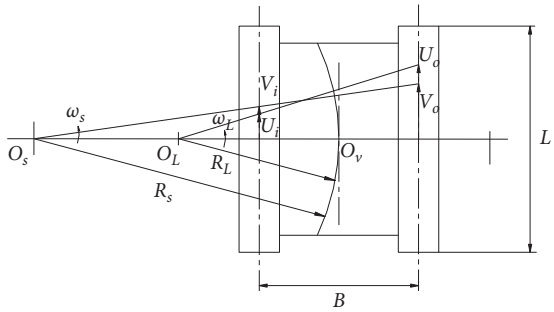


Figure 3: Slip and skid of the tracked vehicle during a steady-state turn.

As the lateral load transfers caused by the centrifugal force during the vehicle's turn are assumed to be absent, the slip and skid of the tracks will cause an offset (from $O_L$ to $O_S$, as illustrated in Figure 3) in the vehicle turning center without any fore-aft offset. The actual turning radius $R_S$ and yaw velocity $\omega_s$ of the tracked vehicle are defined in equations (16) and (17), respectively [12].

$$R_S = \frac{B}{2}\left(\frac{V_o + V_i}{V_o - V_i}\right) = \frac{B}{2}\frac{\left[r\omega_o(1-\sigma_o) + r\omega_i(1-\sigma_i)\right]}{\left[r\omega_o(1-\sigma_o) - r\omega_i(1-\sigma_i)\right]}, \tag{16}$$

$$\omega_S = \frac{V_o - V_i}{B} = \frac{\left[r\omega_o(1-\sigma_o) - r\omega_i(1-\sigma_i)\right]}{B}. \tag{17}$$

Given these equations, the variation of the moment of turning resistance of a tracked vehicle can be calculated—together with its track slip and skid ratios—by substituting equations (5)–(8), (10) and (11), and (16) and (17) into equation (9). Note that the moment of turning resistance of track is a function of the track's slip and skid ratios—at some given soil and track parameters, such as track sprocket angular velocity $\omega_{o,i}$, sprocket radius $r$, track tread $B$, track length $L$, track width $b$, track normal stress $\sigma$, soil cohesion $c$, angle of soil internal shearing friction $\phi$, and soil shear deformation $k$.

*3.1.2. Track Sinkage.* On soft terrains, such as paddy soil, a tracked vehicle sinks deeply into the ground, resulting in track sinkage and subsequent bulldozing effects. Such track sinkage and bulldozing effects should be accounted for in a model. As illustrated in Figure 4, when the vehicle turns, the outer and inner tracks push against the soil in the tracks' lateral direction. According to Rankine's Earth pressure theory [21, 22], the soil in front of the track is brought into a state of passive failure. This phenomenon can be modeled in two dimensions because the ratio of the track length $L$ to the sinkage depth $Z_0$ is large. Furthermore, assuming that the track surface is relatively smooth, the normal pressure exerted by the track on the soil is the major principal stress, and equal to the passive Earth pressure. The bulldozing force $F_p$ acting on the track per unit width can be calculated by integrating the passive Earth pressure over the sinkage depth $Z_0$, from

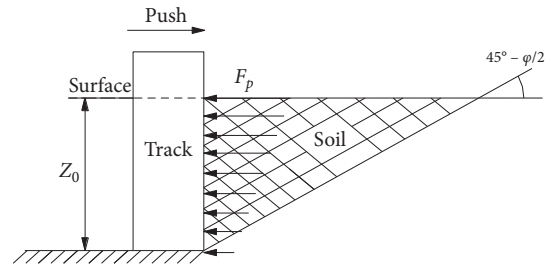


Figure 4: Distribution of track bulldozing resistance at the sinkage depth of $Z_0$.

equation (18). Therefore, the moments of bulldozing resistance $M_{d(o,i)}$ on the outer and inner tracks can be expressed by equation (19).

$$F_p = \int_0^{z_0} \sigma_p dz = \frac{1}{2}\gamma_s z_0^2 N_\varphi + 2cz_0\sqrt{N_\varphi}, \tag{18}$$

$$M_{d(o,i)} = -\int_{-L/2}^{L/2}\left(\frac{1}{2}\gamma_s z_0^2 N_\phi + 2cz_0\sqrt{N_\phi}\right)y_{1,2}\mathrm{d}y_{1,2}, \tag{19}$$

where $\gamma_s$ is soil bulk density, $c$ is the cohesion of soil, $\phi$ is the angle of the soil internal shearing friction, $Z_0$ is the vehicle sinkage depth, and $N_\phi = tan^2(45^\circ + \phi/2)$. Note that the moments of bulldozing resistance $M_{d(o,i)}$ is a function of the track sinkage depth $Z_0$.

*3.1.3. Moment of Turning Resistance.* By considering the effects of track sinkage and track slip and skid, the moments of turning resistance $M_{o,i}$ can be calculated as the resultant of two moments (Figure 2). One of these moments is $M_{T(o,i)}$, which is calculated according to equation (9), and the other is the moment $M_{d(o,i)}$, which is calculated according to equation (19). With these two moments, the resultant moments of turning resistance of a tracked vehicle are as follows:

$$M_{o,i} = M_{T(o,i)} + M_{d(o,i)}. \tag{20}$$

According to the preceding analysis, the moments $M_{T(o,i)}$ are a function of the track slip and skid ratio $\sigma_{o,i}$, and the moments $M_{d(o,i)}$ are a function of the track sinkage depth $Z_0$. By measuring the track slip and slid ratios $\sigma_{o,i}$ as well as the sinkage depth $Z_0$ under given soil conditions, the moments of turning resistance $M_{o,i}$ can be determined.

Furthermore, as illustrated in Figure 2, the equations for the moment of equilibrium of the tracked vehicle with respect to $O_1$ and $O_2$ can be derived to be as follows:

$$\sum M_{o_1} = 0, \quad M_{\mathrm{To}} + M_{\mathrm{do}} - \frac{BT_i}{r_i} = 0, \tag{21}$$

$$\sum M_{o_2} = 0, \quad M_{Ti} + M_{\mathrm{To}} - \frac{BT_o}{r_o} = 0, \tag{22}$$

respectively, where $T_o$ and $T_i$ are the sprocket torques of the outer and inner tracks, respectively, $B$ is the track thread, and $r$ is the sprocket radius.

### 3.2. Field Test

*3.2.1. Vehicle and Sites.* The field test was conducted on October 2018 at Picheng town (119.709°N, 32.115°W), which is located in China's southeast. The mean annual temperature and precipitation were 18.3°C and 1243 mm, respectively. Because the tracks may have different sinkage depths and slip and skid ratios at different soil moisture conditions, the test was conducted on paddy soil (stubble not tilled after harvest) at two different soil water contents (before and after irrigation). The soil texture was classified as clay loam in the topsoil (0–0.2 m depth), and the selected soil parameters are presented in Table 1.

A WORLD 4LZ-4.0 E rubber-tracked combine harvester was used in the test. The vehicle had two turning modes, as depicted in Figure 5. One is a unilateral brake turning mode, and the other is a pivot turning mode. For the unilateral brake turning mode, the brake force is exerted on the inner track, and the turning maneuver is completed by the driving of the outer track. For the pivot turning mode, the inner and outer tracks drive at the same velocities but in the opposite directions. The parameters of the tracked vehicle are presented in Table 2. During the test, the driver was instructed to operate two turning maneuvers at a constant speed, with three replicates. Figure 6 shows the turning maneuver of a combine harvester during the field test.

*3.2.2. Measurement of Track Slip and Skid Ratios and Sprocket Torques.* The *HUADONG DH5905* wireless telemetry analysis system was used in the measurement. The sprocket torques $T_{o,i}$ were measured by pasting four BF120 resistance strain gauges on the surface of the sprocket shaft in the form of a full-bridge circuit, then connected with torque acquisition modules after the calibration. The angular velocities $\omega_{o,i}$ were measured by the *NJC5002 C* hall sensors. Torque acquisition modules and hall sensors were fixed on the tracks, as shown in Figure 7. The test signal was transmitted to a computer through wireless routers for subsequent processing. The track actual velocity $V_{o,i}$ was recorded by GPS which mounted on the vehicle. Subsequently, the track slip and skid ratios were calculated by equations (12) and (13), respectively. The extent of tracked sinkage $Z_0$ was measured directly by a depth meter before the vehicle turned. Undisturbed 100–cm$^3$ soil cores (inner $\Phi = 60$ mm, $H = 34.8$ mm) were sampled in the field before the vehicle turned. The soil parameters $c$, $\phi$, and $K$ were acquired from the Mohr–Coulomb model by conducting soil triaxial tests in the lab. Finally, all soil cores were dried in an oven at 105°C to determine the soil water content $w$ and dry bulk density $\gamma_s$.

## 4. Results and Discussion

*4.1. Variation of Moment of Turning Resistance with Track Slip and Skid Ratios at Different Track Sinkage Depths.* A MATLAB-based simulation was constructed according to the aforementioned equations. equation (20), which governed the moment of turning resistance of the tracked vehicle, was solved. As per Figures 8 and 9 graph, for the two turning modes, the variations of the outer and inner tracks' calculated moments of turning resistance against track sinkage depths and track slip and skid ratios. Crucially, when the vehicle undergoes unilateral brake turning, the inner track is completely stopped by the brake. Thus, the skid ratio of the inner track remains at the maximum value of 1. By contrast, when the vehicle undergoes pivot turning, the inner and outer tracks drive at the same speed; both tracks are slipping, and the slip ratios of the inner and outer tracks are equal.

As illustrated in Figure 8, the simulation results indicated that as the skid ratio of the inner track remained at the maximum value during unilateral brake turning, the moment of turning resistance of the inner track remained almost constant. This small decrease is attributable, according to equation (16), to the increased vehicle turning radius $R_S$ caused by the increase of the slip ratio of the outer track. However, the moment of turning resistance of the outer track decreased with increases in the track slip ratio. As evident in Figure 9, because the slip ratios of inner and outer tracks were equal during pivot turning—meaning that the moment of turning resistance of the two tracks was equal—both tracks decreased as the value of the track slip ratio increased. However, according to Figures 8 and 9, the moment of turning resistance increased with increases in track sinkage depth.

Furthermore, the moment of turning resistance of the inner and outer tracks greatly differed when the vehicle undertook a unilateral brake turning maneuver (Figures 8 and 9), and this difference increased as the track slip ratio increased. By contrast, the outer and inner tracks' moments of turning resistance were the same when the vehicle undertook the pivot turning maneuver. These observations indicate that for the harvester, pivot turning is superior to unilateral brake turning when the tracks' slip ratio is high. The unbalanced moment of turning resistance between the two tracks may cause instability and difficulties when executing the unilateral brake turning maneuver. By contrast, if the moments of turning resistance of the two tracks are equal, the pivot turning maneuver is more easily and stably executed.

*4.2. Corroboration of Model-Predicted Results with Field Test Measurements.* In the paddy field, the tracked harvester was observed while turning in two modes under two different soil water content conditions. Because the moment of turning resistance could not be measured directly, the sprocket torques $T_{o,i}$ that were generated by the inner and outer tracks were measured for comparison with the torques calculated from equations (21) and (22).

Figures 10 and 11 illustrates the comparison between the measured and model-predicted torques under two soil water conditions; both sets of torque values were in good agreement, although the model-predicted values were consistently and slightly higher than the measured ones. This is likely due to our model's exclusion of frictional forces between the tracks' moving parts and additional sliding-sinkage. The track sliding-sinkage effect means an increase of

Table 1: Physicochemical properties of paddy soil (0–0.2 m).

| Texture | | | | WP | Wl |
|---|---|---|---|---|---|
| g $100g^{-1}$ | | | | % | % |
| <0.002 mm | 0.002–0.02 mm | >0.02 mm | Organic matter | Plastic limit | Liquid limit. |
| 40.4 | 38.6 | 21.0 | 3.2 | 26 | 43 |

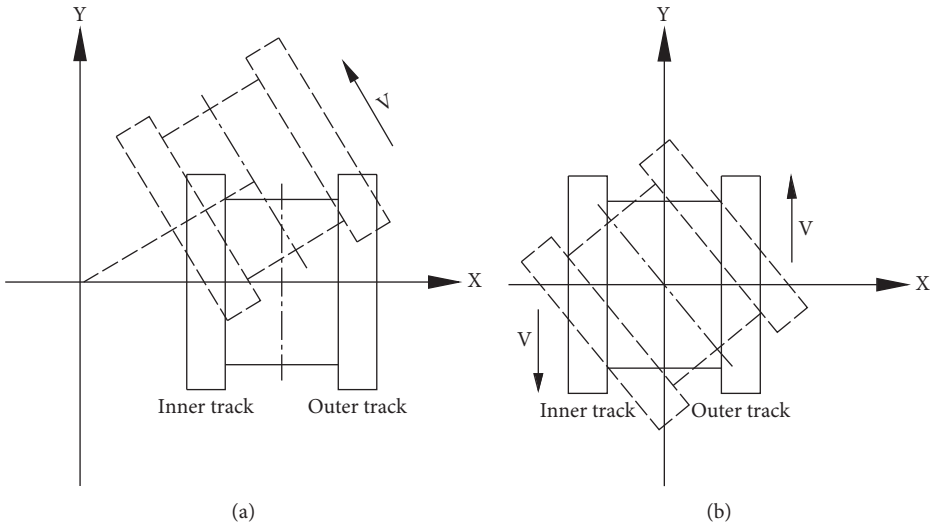


Figure 5: (a) Unilateral brake turning and (b) pivot turning modes of the tracked harvester.

Table 2: Vehicle and soil parameters used in the model simulation.

| | Parameters | Notation | Unit | Value |
|---|---|---|---|---|
| Tracked harvester | Total mass | G | kg | 25,500 |
| | Tread width | B | m | 2.54 |
| | Track length | L | m | 3.8 |
| | Track width | b | m | 0.45 |
| | Sprocket radius | r | m | 0.32 |
| Soil | Cohesion | C | Kpa | 35 |
| | Internal angle of friction | φ | ° | 25 |
| | Shear displacement coefficient | K | m | 0.025 |
| | Soil bulk density | $\gamma_s$ | $g/cm^2$ | 1.5 |

Figure 6: Turning maneuver of WORLD 4LZ-4.0 E combine harvester during the field test.

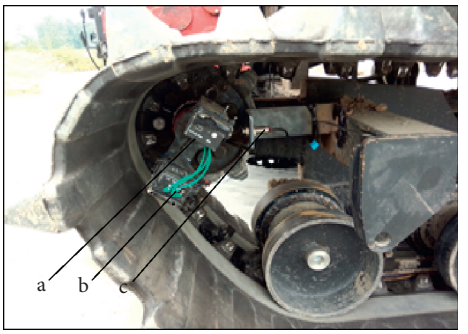


Figure 7: Sprocket torque and angular velocity testing system. (a) Torque acquisition module. (b) Power module bolt. (c) Hall sensor.

vehicle sinkage and motion resistance due to the track sliding [23–25]. In the previous study [24], the track sinkage depth was observed to increase with the growing slip ratio. For the slip ratio range from 0 to 0.33 the sinkage depth increases monotonically, but for 0.33 this increase grows to approximately 60%. Moreover, this effect was found to be

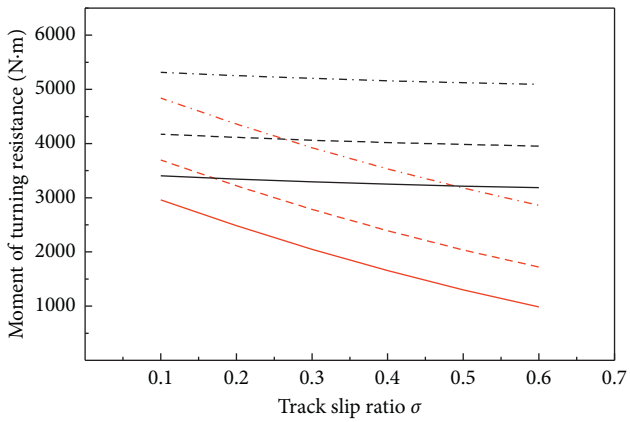


Figure 8: Plot of calculated moments of turning resistance of outer track (black line) and inner track (red line) against track slip ratios at 20 mm (solid line), 40 mm (dashed line), and 70 mm (dotted line) sinkage depths in the unilateral brake turning mode.

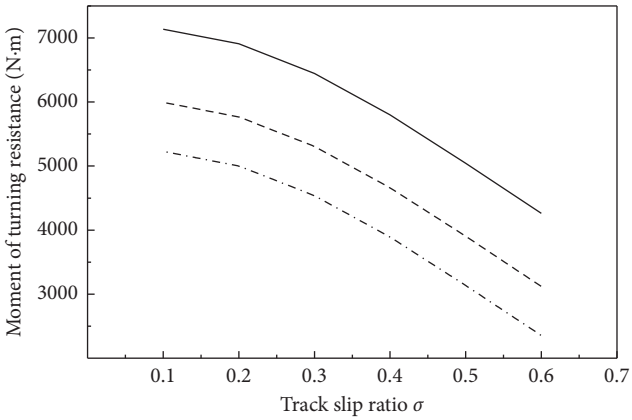


Figure 9: Plot of calculated moments of turning resistance of outer and inner tracks versus track slip ratios at 20 mm (solid line), 40 mm (dashed line), and 70 mm (dotted line) sinkage depths in the pivot turning mode.

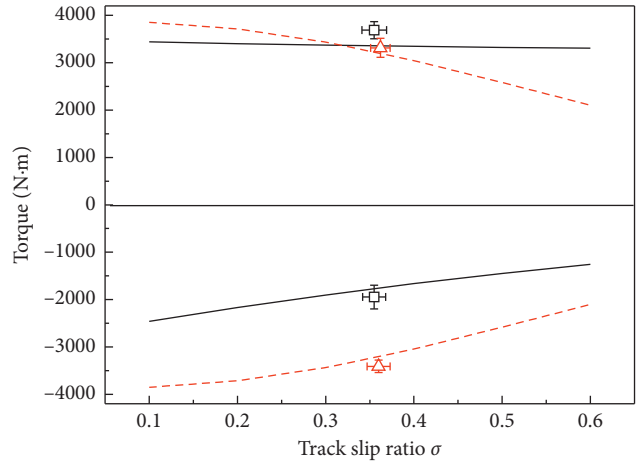


Figure 10: Measured (symbols) and simulated torques (curves) during the unilateral brake turning (measured: black squares; simulated: black solid curves), and pivot turning (measured: red triangles; simulated: red dashed curves) in the paddy field with 28.2% water content. Error bars indicate the standard deviation of the mean.

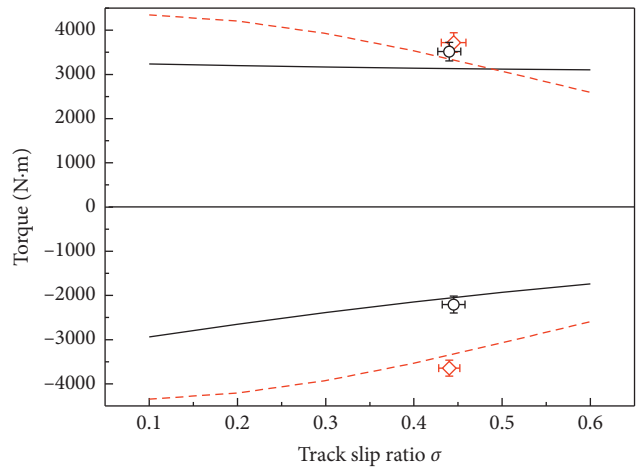


Figure 11: Measured (symbols) and simulated torques (curves) during the unilateral brake turning (measured: black circles; simulated: black solid curves) and pivot turning (measured: red diamonds; simulated: red dashed curves) in the paddy field with 38.9% water content. Error bars indicate the standard deviation of the mean.

greater in the sandy soil than in frictionless clay. In general, the track has a relatively large slip ratio (0.3–0.6) when it turns on the soft terrains [26]; this means that the sliding-sinkage effect should be considered when the tracked vehicle tuns on the soft terrain. Future research will focus on optimizing the theoretical model by accounting for the track sliding-sinkage effect.

Moreover, the error was greater on the inner than on the outer track when the vehicle conducted a unilateral brake turning maneuver (mean 15.3% and 9.5% errors for the inner and outer tracks, respectively). This may be attributable to the transferred load to the inner track. In our model, the vehicle was assumed to turn under steady-state conditions, and the longitudinal and lateral load transfers caused by the centrifugal force were absent. In general, the centrifugal force may cause the fore-aft offset of the vehicle's turning center during the vehicle's turning, resulting in an imbalanced load between two tracks. The track with higher load may have larger amount of sinkage depth than the track on the other side and larger bulldozing resistance on this side. Our future study will focus on developing more accurate models by accounting for additional effects from the vehicle centrifugal force.

The vehicle's running speed may be another factor that affects its turning resistance as well as turning stability. In the previous studies [23, 27], the track rut depth was observed to increase with the running speed. This means that the track sinkage depth increased with the growing running speed, which may result in the increases in the vehicle's bulldozing resistance. Moreover, the centrifugal force may become larger at a high running speed, thus causing more load transfer in the lateral direction, and subsequently aggravating the load imbalance between inner and outer tracks. It

will eventually reduce the vehicle's turning stability. For the tracked harvester, this kind of phenomenon is more likely to occur in unilateral brake turning mode than in pivot turning mode, and more likely to occur in the soil with high water content. The reason is that the simulated turning resistance on the inner track was larger than the outer track when the vehicle conducted unilateral brake turns, and the gap increased gradually with the rising track slip ratio (Figure 8). In other words, the imbalance of the turning resistance between two tracks was aggravated with the increased slip ratio. The study [26] shows that the track usually has a larger slip ratio in the soil with higher water content than in the soil with lower water content. This means that under the unilateral brake turning mode, the stability of the vehicle may reduce at high soil water conditions. By contrast, the turning resistances of the two tracks were equal when the vehicle conducted pivot turns and remained equal as the track slip ratio increased (Figure 9). This allows the vehicle to be more stable and smooth when it turns at high soil water content conditions. The developed model shows the potential not only as a predictor for the vehicle's turning resistance but also as a guide to the selection of appropriate turning modes at different soil conditions to improve the vehicle's turning stability.

In our field test, two soil conditions were selected (i.e., paddy soil with 28.2% and 38.9% water content, respectively) in order to obtain different track slip ratios. However, the slip ratios corresponding to the two soil water content conditions were relatively close, with the value of 0.36 and 0.45 in average, respectively. This to a certain extent reduces the credibility of model validation, although the model-predicted values were in good agreement with the measured ones. It is more convincing to select different terrains with a large difference in the slip ratio for comparison and model validation. More field tests under various types of soil with different water content should be carried out in future studies.

The model's ability to analytically predict the turning resistance of tracked vehicles under different soil conditions at given values of track sinkage depth and track slip and skid ratios means that online prediction of turning resistance is possible–an important building block for future fully autonomous agricultural vehicles. When the classical terrain parameters (e.g., sinkage exponent, cohesion, and internal friction angle) are known, the track sinkage depth can be estimated based on Bekker's theory [28]. To reflect the track sliding-sinkage effect, the sinkage exponent can be expressed as a function of the slip and skid ratio [29–31]. Thus, the accurate estimation of track slip and skid ratio under different soil conditions is crucial for the online prediction. Further research on the prediction of track slip and skid ratios under different soil texture and water content is required. Then the predicted track slip and skid ratio and track sinkage depth can be used to compute the turning resistance in real time.

## 5. Conclusions

We developed a theoretical model for the prediction of the moment of turning resistance of tracked vehicles on soft ground under steady-state conditions. This model accounts for track sinkage and track slip and skid effects. This model is based on principles in Wong's general theory but extends that theory. This model is capable of predicting the moment of turning resistance of tracked vehicles at given values of track sinkage depth, track slip ratio, and track skid ratio. The moment of turning resistance was determined to increase and decrease with increases in the track sinkage depth and track slip and skid ratios, respectively.

A field test was conducted using a tracked harvester; its turning performance on a paddy field was examined. The model-predicted sprocket torque values of the outer and inner tracks closely approximated the measured values obtained in the field test. The experiment demonstrated that the theoretical model accurately predicts the moment of turning resistance of a tracked vehicle. More generally, the model gives insight into the turning performance of tracked vehicles on soft terrain. Future work will focus on further developing the models to account for sliding-sinkage and centrifugal force effect.

## Data Availability

The data used to support the findings of this study are available from the corresponding author upon request.

## Conflicts of Interest

The authors declare that they have no conflicts of interest regarding the publication of this paper.

## Acknowledgments

This research work was supported by the National Key Research and Development Program of China (2016YFD0702004), the Natural Science Foundation of Jiangsu Province (BK20170553), the National Natural Science Foundation of China (51705212), the Graduate Innovative Projects of Jiangsu Province 2015 (KYLX15_1047), and a project funded by the Priority Academic Program Development of Jiangsu Higher Education Institutions (PADP).

## References

[1] G. D. Vermeulen, B. R. Verwijs, and J. J. H. Van den Akker, "Comparison of loads on soils during agricultural field work in 1980 and 2010," *Plant Research International, Rapport*, vol. 501, 2013.

[2] Z. Tang, Y. Li, X. Li et al., "Structural damage modes for rice stalks undergoing threshing," *Biosystems Engineering*, vol. 186, pp. 323–336, 2019.

[3] L. Alakukku, P. Weisskopf, W. C. T. Chamen et al., "Prevention strategies for field traffic-induced subsoil compaction: a review," *Soil and Tillage Research*, vol. 73, no. 1-2, pp. 145–160, 2003.

[4] B. Blunden, R. McBride, H. Daniel, and P. Blackwell, "Compaction of an earthy sand by rubber tracked and tired vehicles," *Soil Research*, vol. 32, no. 5, pp. 1095–1108, 1994.

[5] B. Maclaurin, "A skid steering model with track pad flexibility," *Journal of Terramechanics*, vol. 44, no. 1, pp. 95–110, 2007.

[6] T. Guo, J. Guo, B. Huang, and H. Peng, "Power consumption of tracked and wheeled small mobile robots on deformable terrains-model and experimental validation," *Mechanism and Machine Theory*, vol. 133, pp. 347–364, 2019.

[7] J. Y. Wong, *Theory of Ground Vehicles*, John Wiley & Sons, Hoboken, NJ, USA, 3rd edition, 2008.

[8] J. Guo, L. Ding, H. Gao et al., "Longitudinal skid model for wheels of planetary rovers based on improved wheel sinkage considering soil bulldozing effect," *Journal of Terramechanics*, vol. 74, no. 45–56, 2017.

[9] L. Ding, H. Yang, H. Gao et al., "Terramechanics-based modeling of sinkage and moment for in-situ steering wheels of mobile robots on deformable terrain," *Mechanism and Machine Theory*, vol. 116, pp. 14–33, 2017.

[10] P. D. Ayers, "Environmental damage from tracked vehicle operation," *Journal of Terramechanics*, vol. 31, no. 3, pp. 173–183, 1994.

[11] G. Anousaki and K. J. Kyriakopoulos, "A dead-reckoning scheme for skid-steered vehicles in outdoor environments," in *proccedings of IEEE International Conference on Robotics and Automation*, vol. 1, pp. 580–585, New Orleans, LA, USA, January 2004.

[12] W. Steeds, "Tracked vehicle," *Automobile Engineer*, vol. 40, p. 526, 1950.

[13] M. Kitano and H. Jyozaki, "A theoretical analysis of steerability of tracked vehicles," *Journal of Terramechanics*, vol. 13, no. 4, pp. 241–258, 1976.

[14] W. Ehlert, B. Hug, and I. C. Schmid, "Field measurements and analytical models as a basis of test stand simulation of the turning resistance of tracked vehicles," *Journal of Terramechanics*, vol. 29, no. 1, pp. 57–69, 1992.

[15] J. E. Crosheck, *Skid Steering of Crawlers*, SAE International, Warrendale, PA, USA, 1975.

[16] C. F. Chiang, *Handling Characteristics of Tracked Vehicles on Non-deformable Surfaces*, Carleton University, Ottawa, Canada, 1999.

[17] J. Y. Wong and C. F. Chiang, "A general theory for skid steering of tracked vehicles on firm ground," *Proceedings of the Institution of Mechanical Engineers, Part D: Journal of Automobile Engineering*, vol. 215, no. 3, pp. 343–355, 2001.

[18] S. Al-Milli, L. D. Seneviratne, and K. Althoefer, "Track-terrain modelling and traversability prediction for tracked vehicles on soft terrain," *Journal of Terramechanics*, vol. 47, no. 3, pp. 151–160, 2010.

[19] S. Al-Milli, K. Althoefer, and L. D. Seneviratne, "Maneuverability performance of tracked vehicles on soft terrains," in *Proceedigs of International Conference on Intelligent Robots and Systems*, pp. 107–112, IEEE, Piscataway, NJ, USA, September 2008.

[20] Z. Janosi and B. Hanamoto, "The analytical determination of drawbar pull as a function of slip for tracked vehicles in deformable soils," in *Proceeding of the First International Conference on Terrain-Vehicle Systems*, ISTVS, Turin, Italy, June 1961.

[21] Y. S. Fang, T. J. Chen, and B. F. Wu, "Passive earth pressures with various wall movements," *Journal of Geotechnical Engineering*, vol. 120, no. 8, pp. 1307–1323, 1994.

[22] J. M. Duncan and R. L. Mokwa, "Passive earth pressures: theories and tests," *Journal of Geotechnical and Geoenvironmental Engineering*, vol. 127, no. 3, pp. 248–257, 2001.

[23] K. Liu, P. Ayers, H. Howard, and A. Anderson, "Lateral slide sinkage tests for a tire and a track shoe," *Journal of Terramechanics*, vol. 47, no. 6, pp. 407–414, 2010.

[24] M. Lyasko, "Slip sinkage effect in soil-vehicle mechanics," *Journal of Terramechanics*, vol. 47, no. 1, pp. 21–31, 2010.

[25] L. Ding, J. Guo, B. Yan et al., "Longitudinal skid experimental investigation for wheels of planetary exploration rovers," *Journal of Mechanical Engineering*, vol. 51, no. 18, p. 99, 2015.

[26] C. Wei, "Study on the Skid-Steered of Tracked Vehicles," Doctoral Thesis, Beijing Institute of Technology, Beijing, China, 1980.

[27] K. Liu, P. Ayers, H. Howard, and A. Anderson, "Influence of soil and vehicle parameters on soil rut formation," *Journal of Terramechanics*, vol. 47, no. 3, pp. 143–150, 2010.

[28] M. G. Bekker, *Theory of Land Locomotion*, University of Michigan Press, Ann Arbor, Michigan, USA, 1956.

[29] J. Guo, T. Guo, M. Zhong et al., "In-situ evaluation of terrain mechanical parameters and wheel-terrain interactions using wheel-terrain contact mechanics for wheeled planetary rovers," *Mechanism and Machine Theory*, vol. 145, p. 103696, 2020.

[30] J. Guo, H. Gao, H. Ding, T. Guo, and Z. Deng, "Linear normal stress under a wheel in skid for wheeled mobile robots running on sandy terrain," *Journal of Terramechanics*, vol. 70, pp. 49–57, 2017.

[31] Z. Liu, J. Guo, L. Ding, H. Gao, T. Guo, and Z. Deng, "Online estimation of terrain parameters and resistance force based on equivalent sinkage for planetary rovers in longitudinal skid," *Mechanical Systems and Signal Processing*, vol. 119, pp. 39–54, 2019.